PHYSICAL REVIEW B VOLUME 58, NUMBER 19 15 NOVEMBER 1998-I

Diffusion mechanisms of a Si adatom on H-terminated Si(100) surfaces

Sukmin Jeong and Atsushi Oshiyama
Institute of Physics, University of Tsukuba, Tennodai, Tsukuba 305, Japan

(Received 24 December 1997; revised manuscript received 24 July 1998)

We present features in the adsorption and diffusion of a Si adatom on H-terminated Si(100) surfaces based on first-principles total-energy calculations. We find that the adatom spontaneously substitutes for a H atom upon adsorption. The resulting diffusion species on the surface is no longer a single atom and a typical approach based on a single potential energy surface is invalid. As an alternative, we trace the diffusion pathways of the adatom-H unit, simultaneously examining the effect of H release and capture by the adatom. Extensive investigations on the 2×1 phase show that the adatom releases the H atom bonded to it and captures another H atom as it migrates on the surface. In addition, the adatom penetrates into the surface, breaking a surface backbond. This results in exchange between the adatom and a surface Si atom. The mechanisms of H release and capture and of adatom exchange are also expected on other phases of the H-terminated Si(100) surfaces. [S0163-1829(98)07943-0]

I. INTRODUCTION

Diffusion is one of the basic processes on surfaces that plays important roles in epitaxial growth and that determines morphology of resulting thin films.[1] It is greatly affected by states of surfaces, e.g., impurities, defects, adsorbates, and so on. Introduction of foreign atoms onto surfaces also modifies the diffusion of adsorbates and results in a remarkable change in the morphology and epitaxial growth. For example, hydrogen adsorption on Si surfaces has been studied extensively because of its possible application to nanoscale devices and as a means of understanding interactions between semiconductors and simple H atoms. [2–12]

Many previous studies using molecular beam epitaxy and chemical vapor deposition have reported interesting features produced by H atoms in epitaxial growth.[2–10] In H-assisted Si homoepitaxies, Si islands become less anisotropic in shape and the island density increases compared with the case on the clean surface.[5,9,10] In their recent transmission electron microscopy study on Ge heteroepitaxy on Si surfaces, Sakai and Tastumi found that H works as a surfactant during growth, suppressing island formation of Ge on the substrate.[7] Using medium-energy ion scattering, Copel and Tromp observed that the growth behavior of Si overlayers on Si surfaces strongly depends on H coverage.[8] Little is known, however, about microscopic processes, adsorption and diffusion processes of an adatom, which lead to changes in the morphology and growth of the overlayers.

A typical approach to the diffusion problem of an adatom on surfaces is to map a potential energy surface (PES) as a function of the lateral coordinates of the adatom.[13–15] The picture of diffusion is that the adatom hops among metastable sites via transition sites on the PES. The diffusion barrier is determined by the energy difference between the minimum and transition points along each pathway. In the present case, however, we show that the Si adatom substitutes for a H atom with no energy barrier on the H-terminated Si(100) surfaces.[16] Because of the spontaneous formation of an adatom-H unit or an adatom-H_2 unit, the diffusion species is no longer a Si adatom itself. This implies that a single PES is not enough to describe correct diffusion processes of the adatom.

In this paper, we propose diffusion mechanisms of a Si adatom on the H-terminated Si(100) surfaces based on the total-energy electronic-structure calculations within the local density approximation (LDA). We find spontaneous substitutional adsorption on all the 2×1, 3×1, and 1×1 phases[17] of the H-terminated Si(100) surfaces. On the 2×1 phase, a H atom is bonded to the Si adatom in the resulting stable geometry. We discuss the limitations of the PES in describing the adatom diffusion. We also find that at the same lateral position of the adatom, the total energy depends on the number of H atoms attached to the adatom. We thus follow the diffusion pathways of the adatom-H unit, and simultaneously examine the effects of the H release and capture by the adatom. From the extensive investigations on the 2×1 phase, we find that the adatom diffuses via a complicated way where the H *release* and *capture* by the adatom and the *exchange* of the adatom with a surface Si atom are involved. The obtained activation energies for adatom diffusion parallel and perpendicular to the substrate dimer rows are 0.7 and 1.0 eV, respectively. These values are rather comparable to those of the clean Si(100) surface, but the diffusion mechanisms of the two surfaces are completely different. The diffusion mechanisms of H release and capture and adatom exchange are also expected on the 1×1 and 3×1 phases since the transition-state geometries of the Si adatom on the two phases are quite similar to those of the 2×1 phase. On the 1×1 and 3×1 phases, the diffusion becomes isotropic and the calculated barriers are 2.7 and 2.2 eV, respectively. These dramatic increases in diffusion barriers are consequences of the stable adsorption geometries in which the adatom-H_2 unit is formed.

II. CALCULATIONAL METHOD

All calculations have been performed using norm-conserving pseudopotentials,[18] the LDA (Ref. 19) for the exchange correlation energy, and the conjugate-gradient minimization technique as reported elsewhere.[20] The surface is

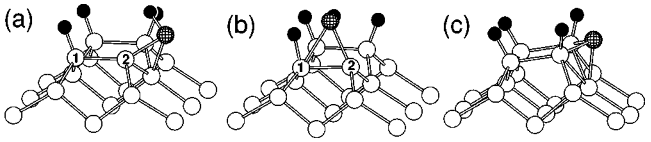

FIG. 1. (a) Stable, (b) metastable, and (c) saddle-point adsorption geometries on the 2×1 monohydride phase. The position of the adatom is (a) A, (b) E, or (c) B as in Fig. 3 of Ref. 16. Meshed, filled, and open circles denote a Si adatom, H atoms, and Si atoms, respectively.

simulated by a repeating slab model in which 5 Si atomic layers and an 8.76 Å vacuum region are included. The bottom of the slab has a bulklike structure with each Si atom saturated by two H atoms. On the top of the slab, which simulates the real surface, a H adlayer plus a Si adatom is considered. The size of the unit cell in the lateral directions is $p(\sqrt{8}\times\sqrt{8})R45°$ for the 2×1 and 1×1 phases, and $p(3\times3)$ for the 3×1 phase. It is found that the 4 k points in the surface Brillouin zone (SBZ), and the 8-Ry cutoff energy in the plane wave basis set are necessary to obtain converged results.[16] We use a local potential for H, while s and p nonlocality is taken into account for Si. The geometry optimization has been performed for all atoms except for the bottommost H and Si atoms. In the optimized geometries the remaining forces acting on the atoms are less than 0.005 Ry/Å.

In order to check the validity of our parameters, we have carried out calculations for the 2×1 monohydride, the 1×1 canted-dihydride, and the 3×1 monohydride plus dihydride Si(100)-H surfaces. We have used a $p(6\times1)$ unit cell that can accommodate all three structures. We have chosen 6 k points in the SBZ so that we have a similar k point density to that in the $p(\sqrt{8}\times\sqrt{8})R45°$ unit cell with 4 k points. The calculated Si-H bond lengths are all approximately 1.51 Å, regardless of phases. The Si-Si dimer bond lengths in the 2×1 and 3×1 phases are 2.40 and 2.41 Å, respectively. These structural parameters agree well with previous results.[17] We have also investigated the relative stability of each phase as a function of the H chemical potential μ_H. We have found that as the H chemical potential increases, the transitions from the 2×1 phase to the 3×1 phase and then from the 3×1 phase to the 1×1 phase occur at $\mu_H = -0.22$ eV and -0.01 eV, respectively (The reference of μ_H is the chemical potential at which the formation energy of SiH_4 is equal to zero). These values are comparable to previous studies, -0.24 and -0.09 eV,[17] and -0.27 and -0.01 eV.[21]

III. RESULTS

A. Spontaneous substitutional adsorption

Figure 1 shows the (meta)stable adsorption geometries on the 2×1 monohydride surface. The structures do not have any symmetry either in the location of the adatom or in the adatom-H bond direction. One of the most striking features in these geometries is substitutional adsorption: the Si adatom is directly bonded to a dimer atom (Si2), while the H atom, originally bonded to Si2, now forms a bond with the adatom. The adatom in Fig. 1(a) has three bonds: with the H atom, Si2, and a subsurface Si atom with bond lengths of 1.54, 2.25, and 2.59 Å, respectively. The Si1-Si2 dimer bond length (2.40 Å) is not affected by the presence of the adatom. Of interest is that the subsurface Si atom bonded to the Si adatom is fivefold coordinated. This is a manifestation of floating bonds originally postulated in amorphous Si.[22] In Fig. 1(b), the adatom also has three coordinations with the H, and the two Si dimer atoms (Si1 and Si2). The corresponding bond lengths are 1.55, 2.70, and 2.34 Å, respectively. The Si1-Si2 dimer bond length is 2.39 Å. In this way, the number of dangling bonds is reduced as much as possible in both (a) and (b), and the structures are thus stabilized. The adsorption energies of (a) and (b) are 3.2 and 3.15 eV, respectively.[23] This similarity in energetics is understandable by counting the number of dangling bonds, although their structures are completely different.

The substitutional adsorption takes place without any energy barrier.[16] The spontaneous substitution provides an important clue to the surfactant effect of H atoms.[7] It is essential that a surfactant atom terminate the growth front during epitaxy, to lower the surface free energy, and to change the diffusion behaviors.[14] In the present system, the reasons for the spontaneous substitutional adsorption are the small atomic radius of H atoms and the strong covalency of group IV atoms. We therefore expect that substitutional adsorption of the adatom also occurs in heteroepitaxy of Ge on Si(100)-H. In that case the crystal growth front is always terminated by H. We are not aware of direct experimental evidence of this interesting phenomenon yet, but it has been reported that H atoms easily segregate to the surface in Si homoepitaxy.[8]

B. Potential energy surface for the 2×1 phase

The (spontaneous) substitutional adsorption takes place on many sites. It is shown well on the PES of the 2×1 monohydride surface (Fig. 3 in Ref. 16). At most sites, the adatom is bonded to a *single* hydrogen atom. At a site that is equidistant from two dimer atoms (the left panel of Fig. 3 in Ref. 16), however, the adatom has bonds with *two* H atoms that were originally attached to Si1 and Si2 (Fig. 1). After all, the total energy surface is composed of three parts, in each of which the adatom is bonded with none, one, and two H atoms, respectively. This feature makes it complex to apply the PES directly to the diffusion problem.

The PES of Fig. 3 in Ref. 16 nevertheless provides important information on diffusion of the Si adatom on the 2×1 monohydride Si(100) surface. The energy surface may lead to a diffusion pathway parallel to the substrate dimer rows along $A^1B^0A^1C^1A^1\ldots$ passing through saddle point B^0, and a pathway perpendicular to the rows along $A^1D^0A^1E^1A^1\ldots$ passing through saddle point D^0. (Hereafter, we use these notations to designate adatom geometries. The superscript of the adatom site is the number of H atoms bonded to the adatom.) In both pathways, geometries where the adatom has no H (B^0 and D^0) become saddle points. This means that H release and capture (by the adatom) is involved during adatom diffusion. This aspect will be discussed in depth in the next subsection.

Furthermore, multistability characteristics are encountered for the PES: At the same lateral coordinates of the

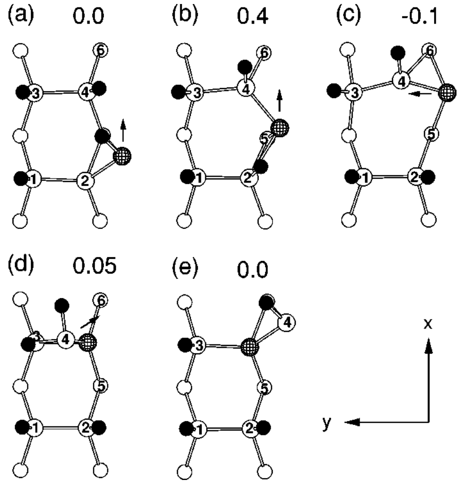

FIG. 2. Diffusion pathway of an adatom along the dimer rows. (a) and (e) are equivalent to Fig. 1(a), and (d) is to Fig. 1(b). Meshed, filled, and open circles denote a Si adatom, H atoms, and Si atoms, respectively. The arrow in each figure indicates the direction of adatom [or a dimer atom in (d)] migration toward the next stage. The value shown above each structure is its total energy in eV with respect to the monohydride geometry at site *A*.

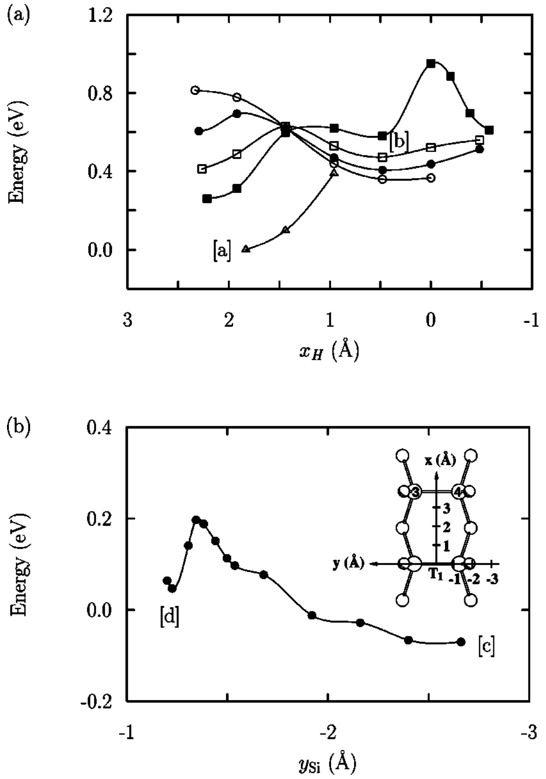

FIG. 3. (a) Total energy variation as a function of the *x* coordinate of the H atom bonded to the adatom (x_H). Each curve corresponds to a different *x* position of the Si adatom (open triangles: 0.96 Å, filled squares: 1.92 Å, open squares: 2.08 Å, filled circles: 2.24, and open circles: 2.40 Å). Refer to the inset in (b) for the arrangement of the coordinates. For $x_{Si}=0.96(1.92)$ Å, the adatom is located around $A(B)$. (b) Total energy variation as a function of the *y* coordinate of the adatom. Letters a, b, c, and d in square brackets correspond to the geometries (a), (b), (c), and (d) in Fig. 2. Solid curves in all plots are to guide the eye.

adatom, the total energy varies depending on the number of H atoms attached to the adatom. When the adatom is located around site *B*, for example, total energies are 0.7 eV, 0.2 eV, and -0.7 eV, for B^0, B^1, and B^2, respectively. For a complete understanding of adatom diffusion, all energy surfaces of the three species, which are connected through release or capture of H atoms, are required.[24]

C. Diffusion along the dimer rows

We now consider the diffusion of the adatom along the dimer rows. Instead of investigating all the PESs (which may exceed the current computational resources), diffusion pathways of the *adatom-H* unit are traced from site *A* along the dimer rows, and at the same time, H release from the diffusion species is thoroughly investigated for several adatom positions. It is reasonable to take A^1 as the starting point since it is the lowest-energy geometry that can be reached upon adsorption without any energy barrier. Based on this approach, it has been found that the following four-stage process is a highly favorable diffusion pathway (Fig. 2): (1) migration of the adatom-H unit and release of the H atom to a dimer atom (Si2) [(a) and (b)], (2) penetration of the adatom into the surface [(b) and (c)], (3) exchange between the adatom and a surface Si atom (Si4) [(c) and (d)], and (4) migration of a new adatom [(d) and (e)].

(1) Release of a H atom: Figure 3(a) shows the energetics of H release from the adatom. The curves are energy variations as a function of the *x* coordinate of the H atom (x_H) bonded either to the Si adatom or to the Si dimer atom [see the inset of Fig. 3(b) for the *xy* coordinates]. Different curves correspond to different *x* positions of the adatom (x_{Si}). Each curve has been obtained from a series of constrained minimization calculations where x_{Si} is fixed and then the minimization is repeated for several x_H in order to obtain the activation energy for H release. When the adatom is located at *A* (corresponding to $x_{Si}=0.96$ Å), H release is of course unfavorable [triangular symbols in Fig. 3(a)]. In fact, it is impossible to get a stable A^0 geometry. As the adatom migrates in the *x* direction, i.e., x_{Si} increases, the total energy increases since the adatom-Si2 bond weakens, and since the two H atoms (bonded to the adatom and Si4) repel each other. It can be seen that the energy barrier for H release depends on the adatom position; it decreases gradually with increase in x_{Si}. At $x_{Si}=2.40$ Å, the adatom-H bond is at last broken spontaneously (open circles). It is evident from Fig. 3(a) that the process in which the adatom migrates with a H atom to the $x_{Si}=2.08$ Å position (open-square curve) followed by H release at the position is energetically favorable.

(2) Penetration of the adatom: The structure after H release is depicted in Fig. 2(b).[25] Of note is that the Si4-Si5 backbond is nearly broken (the distance is 3.19 Å).[26] As the adatom moves further in the *x* direction, the total energy decreases monotonically until the adatom arrives at site *C* [Fig. 2(c)]. One of its interesting features is that the adatom penetrates into the surface, pushing the dimer atom (Si4) outward (Si4 is 0.51 Å higher than the adatom). The energy of (c) is lower than that of (a) by 0.1 eV. The structure is stable since the adatom has three bonds: with a Si dimer atom (Si4), and two subsurface atoms (Si5 and Si6) (the corresponding bond lengths are 2.24, 2.36, and 2.64 Å, respectively). Note that geometry (c) cannot be reached through direct adsorption.

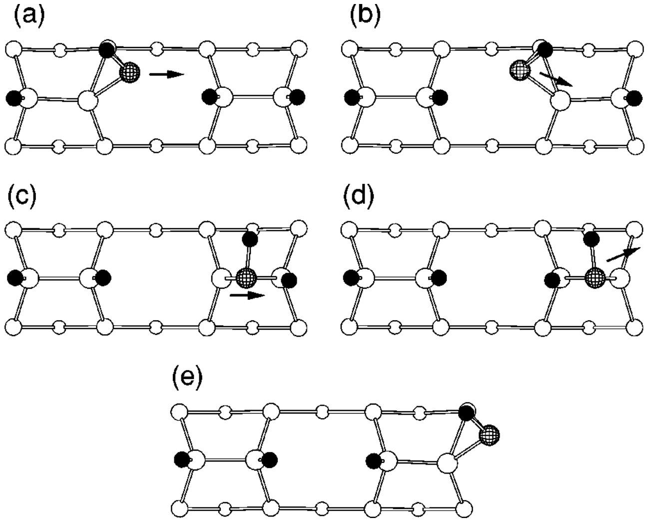

FIG. 4. Diffusion pathway of an adatom perpendicular to the dimer rows. The arrow in each figure indicates the direction of adatom migration toward the next stage. Meshed, filled, and open circles denote a Si adatom, H atoms, and Si atoms, respectively.

(3) Exchange of the adatom: The adatom does not continue its forward migration since the energy cost is very high. Instead it turns to the y direction [arrow in Fig. 2(c)]. The energy change during this process is shown in Fig. 3(b). This has been calculated by optimizing all coordinates except the y coordinates of the adatom and the dimer atom Si3. The activation energy for the exchange process is only 0.3 eV. It is expected that the energy cost of the process in Figs. 2(c)–2(d) is small since it does not induce significant changes in bonding configuration. The resulting structure in Fig. 2(d) is the same as E^1 in Fig. 1(b) except for exchange between the adatom and a dimer atom.

(4) Migration of the new adatom: The final step is that the new adatom Si4 overcomes the 0.5-eV barrier from E to A. During this step, the adatom moves with a H atom. This completes the adatom diffusion cycle.

The rate-determining process among the above four stages is H release, with an energy barrier of 0.7 eV [between Figs. 2(a) and 2(b)]. We thus regard this value as the adatom diffusion barrier parallel to the dimer rows ($Q_\parallel$) on the monohydride Si(100) surface.

D. Diffusion perpendicular to the dimer rows

We expect a similar mechanism for adatom diffusion perpendicular to the dimer rows. A series of structures that appear during adatom diffusion is shown in Fig. 4: by symmetry, geometries (a), (b), and (e) are equivalent and are depicted by A^1; geometries (c) and (d) are also equivalent (E^1). We find that H release and capture are involved in the processes between (a) and (b), and between (c) and (d). As in the previous subsection, the total energy has been calculated as a function of y coordinates of the Si adatom and the H atom bonded to the adatom. First, as is clear from Fig. 4, the microscopic processes between (b) and (c) and between (d) and (e) are identical to the process between (d) and (e) in Fig. 2. In this case, the rate-determining process is the migration from (a) to (b), accompanied by H release and capture. The energy cost is calculated to be 1.0 eV, which is the activation energy for adatom diffusion perpendicular to the dimer rows ($Q_\perp$).

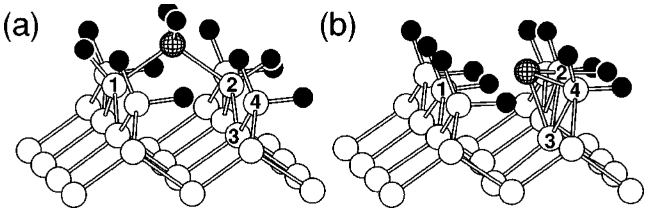

FIG. 5. (a) Stable and (b) saddle-point geometries of a Si adatom on the 1×1 canted dihydride phase. Meshed, filled, and open circles denote a Si adatom, H atoms, and Si atoms, respectively.

The obtained barriers for adatom diffusion ($Q_\parallel = 0.7$ and $Q_\perp = 1.0$ eV) are quite similar to those on the clean Si(100) surface ($Q_\parallel = 0.6$ and $Q_\perp = 1.0$ eV),[13,27] but the present diffusion processes contain rich features that sharply contrast the clean surface case, where the adatom diffuses following a single PES.[13]

E. Diffusion on the 1×1 and 3×1 phases

Spontaneous substitutional adsorption takes place on both the 1×1 canted dihydride phase and the 3×1 monohydride plus dihydride phase. The stablest geometries are displayed in Figs. 5(a) and 6(a). The adsorption energy of the 1×1 phase is 5.3 eV, much larger than the value of the 2×1 phase (3.2 eV). This stability comes from the saturation of the adatom dangling bonds and the bulklike configuration around the adatom. The Si1-adatom-Si2 and H-adatom-H bond angles are 108.0° and 109.2°, respectively. These are close to the value in bulk Si, 109.5°. It is worth noting that the present adsorption energy is nearly equal to the cohesive energy of bulk Si. Figure 5(b) shows one of the saddle-point geometries on the PES of the 1×1 surface, which is 2.7 eV higher than that of the stablest geometry. No H atom is attached to the adatom in this geometry. We thus expect that H release and capture are involved in adatom diffusion. The Si2-Si3 and Si4-Si3 backbond strengths become substantially weak (bond length: 2.82 Å for both cases). Exchange of the diffusion species is also possible since the adatom can easily penetrate into the surface through the weak backbonds. Although complicated microscopic processes are involved, such as H release and capture and exchange between the adatom and other surface atoms, it is likely that the energy cost for each process is at most 1 eV, from the computations on the 2×1 phase. The value 1 eV is much smaller

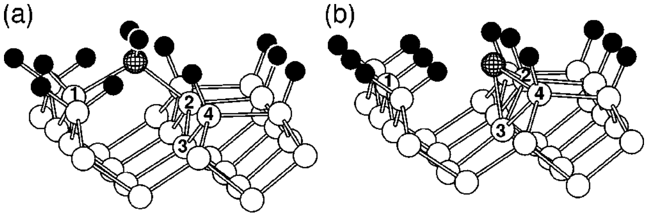

FIG. 6. (a) Stable and (b) saddle-point geometries of a Si adatom on the 3×1 monohydride plus dihydride phase. Meshed, filled, and open circles denote a Si adatom, H atoms, and Si atoms, respectively.

than the simple total-energy difference between the geometries Figs. 5(a) and 5(b). We thus provisionally conclude that the diffusion barrier is close to the energy difference 2.7 eV. For the other principal direction for adatom diffusion, we again obtain a 2.7-eV barrier. This isotropic diffusion is due to a common geometric feature (i.e., two dangling bonds) in the two saddle-point geometries.

For the 3×1 phase, the adsorption energy of the stablest geometry [Fig. 6(a)] is calculated to be 4.8 eV, smaller than that of the 1×1 phase. This results from the strain around the adatom and neighboring Si atoms. The Si1-adatom-Si2 and H-adatom-H bond angles are 112.7° and 109.1°, respectively. One of the saddle-point geometries shown in Fig. 6(b) has a 2.2 eV higher energy than the stablest geometry. We regard the 2.2-eV energy difference as the diffusion barrier. This is smaller than on the 1×1 phase, but still much larger than on the monohydride phase. By the same reasoning, it may be expected that adatom diffusion includes H release and capture, and adatom exchange. Again the diffusion is isotropic. The implication for the dramatic increases in diffusion barriers for high H coverage has been discussed in Ref. 16.

IV. DISCUSSION

A. Exchange process in diffusion

From the present calculations, it is clear that the occurrence of the adatom exchange is ascribed to the saturation of surface dangling bonds by H atoms. In the saddle-point geometries, the overcoordination of surface Si atoms due to the presence of the adatom results in weakening of surface backbonds. The backbond lengths increase significantly around the adatom: 22, 20, and 21% longer than the bulk value on the 2×1, 1×1, and 3×1 phases [refer to Figs. 1(c), 5(b), and 6(b)]. It is thus likely that the adatom can easily penetrate into the surface through these regions. Another role of H atoms is that they stabilize the adatom-penetrated geometry as seen in Fig. 2(c). On the clean surface, however, the configuration Fig. 1(c) is the stablest while the configuration Fig. 2(c) is unstable since two additional dangling bonds (of Si2 and Si4) are produced in the latter case.

Unlike metal systems,[28–32] discussion of the exchange diffusion mechanisms in semiconductor systems has been limited so far. A decade ago, Pandey proposed the exchange mechanism for the self-diffusion in bulk Si based on his first-principles calculations.[33] Roland and Gilmer observed exchange events between an adatom and a surface Si atom using a classical molecular dynamics (MD) simulation.[15] A recent MD study using a similar method reported adatom penetration into the H-terminated Si(100)2×1 and 1×1 surfaces.[34] But these MD studies discussed neither the detailed (exchange or penetration) processes nor the activation energy. On the other hand, we know of no experimental data published for the exchange processes on semiconductor surfaces. When Ge, electronically similar to Si, is deposited on hydrogenated Si surfaces, the diffusion mechanisms proposed here will still be operative, and many mixed dimers of Si and Ge atoms will be produced as a result [refer to Figs. 2(d) and 2(e)]. From the surface energy context, such mixed dimers are energetically unfavorable. They are observed for Ge deposition on clean Si(100) surfaces, however.[35,36] It is inferred from the present results that the H atom on Si surfaces enhances the exchange processes in diffusion and promotes the generation of mixed dimers in Ge deposition.

B. Dynamic aspects of diffusion on the 2×1 phase

Finally, we consider the effect of dihydride geometry on adatom diffusion on the 2×1 phase. We have found that when the adatom is located at site *B* and above the center of a dimer axis, stable adatom-H_2 units are formed. Both that have similar total energies are stabler than A^1 by 0.7 eV. When the adatom is trapped on the geometry, the barrier will become at least 1.4 and 1.7 eV for diffusion parallel and perpendicular to the dimer rows, respectively.[37] This means that the adatom-H_2 unit is nearly immobile compared to the adatom-H unit.

In contrast to the 1×1 and 3×1 phases, formation of an adatom-H_2 unit requires an activation energy. Although the adatom will eventually favor the dihydride structure in equilibrium, it is necessary to consider dynamic features for a complete understanding of adatom diffusion, because the diffusion coefficient is composed of a temperature-independent prefactor and an Arrhenius part. Whichever channel the adatom chooses, the diffusion mechanisms of H release and capture, and adatom exchange are expected to work.

V. SUMMARY

In summary, we have presented LDA calculations providing a detailed picture of adsorption and diffusion of a Si adatom on hydrogenated Si(100) surfaces. We have found that the adatom spontaneously substitutes for the H atom, and that the typical potential energy surface does not accurately reflect the adatom diffusion in the present systems due to the spontaneous substitutional adsorption. Based on an alternative approach, in which the diffusion pathways of the adatom-H unit are traced, we have proposed diffusion mechanisms of the adatom on the 2×1 monohydride surface: i.e., H release and capture, and adatom exchange. We have argued that similar mechanisms are also applied to the 1×1 and 3×1 phases from consideration of transition-state geometries. The calculated diffusion barriers for both phases increase significantly compared to the 2×1 phase, due to the stable adatom dihydride geometries. The calculated results offer a firm theoretical framework for understanding microscopic mechanisms of epitaxial growth on Si(100)-H.

ACKNOWLEDGMENTS

This work was supported in part by the Japan Society for the Promotion of Science under Contract No. RFTF96P00203 (JSPS Research for the Future Program in the Area of Atomic Scale Surface and Interface Dynamics under the project of ‘‘The First-Principles Quantum Theoretical Approach and Microscopic Simulations’’). Computations were partly done on a VPP500 at the Institute for Solid State Physics, University of Tokyo.

[1] M. G. Lagally, Phys. Today **46**, 11 (1993), and references therein.

[2] J. J. Boland, Adv. Phys. **42**, 129 (1993), and references therein.

[3] M. Copel and R. M. Tromp, Appl. Phys. Lett. **58**, 2648 (1991).

[4] K. Sumitomo, T. Kobayashi, F. Shoji, K. Oura, and I. Katayama, Phys. Rev. Lett. **66**, 1193 (1991).

[5] D.-S. Lin, E. S. Hirschorn, T.-C. Chiang, R. Tsu, D. Lubben, and J. E. Greene, Phys. Rev. B **45**, 3494 (1992).

[6] M. J. Bronikowski, Y. Wang, and R. J. Hamers, Phys. Rev. B **48**, 12 361 (1993).

[7] A. Sakai and T. Tatsumi, Appl. Phys. Lett. **64**, 52 (1994).

[8] M. Copel and R. M. Tromp, Phys. Rev. Lett. **72**, 1236 (1994).

[9] J. E. Vasek, Z. Zhang, C. T. Salling, and M. G. Lagally, Phys. Rev. B **51**, 17 207 (1995).

[10] M. Fehrenbacher, J. Spitzmüller, U. Memmert, H. Rauscher, and R. J. Behm, J. Vac. Sci. Technol. A **14**, 1499 (1996).

[11] J. W. Lyding, T.-C. Shen, J. S. Hubacek, J. R. Tucker, and G. C. Abeln, Appl. Phys. Lett. **64**, 2010 (1994).

[12] T. Hashizume, S. Heike, M. I. Lutwyche, S. Watanabe, K. Nakajima, T. Nishi, and Y. Wada, Jpn. J. Appl. Phys., Part 2 **35**, L1085 (1996).

[13] G. Brocks, P. J. Kelly, and R. Car, Phys. Rev. Lett. **66**, 1729 (1991).

[14] B. D. Yu and A. Oshiyama, Phys. Rev. Lett. **72**, 3190 (1994).

[15] C. Roland and G. H. Gilmer, Phys. Rev. B **46**, 13 428 (1992).

[16] S. Jeong and A. Oshiyama, Phys. Rev. Lett. **79**, 4425 (1997).

[17] For details of the three phases, see, e.g., J. E. Northrup, Phys. Rev. B **44**, 1419 (1991).

[18] N. Troullier and J. L. Martins, Phys. Rev. B **43**, 1993 (1991).

[19] D. M. Ceperley and B. J. Alder, Phys. Rev. Lett. **45**, 566 (1980).

[20] O. Sugino and A. Oshiyama, Phys. Rev. Lett. **68**, 1858 (1992); M. Saito, O. Sugino, and A. Oshiyama, Phys. Rev. B **46**, 2606 (1992); B. D. Yu and A. Oshiyama, Phys. Rev. Lett. **71**, 585 (1993).

[21] A. Vittadini, A. Selloni, R. Car, and M. Casarin, Phys. Rev. B **46**, 4348 (1992).

[22] S. T. Pantelides, Phys. Rev. Lett. **57**, 2979 (1986).

[23] In calculating adsorption energies, we neglect the spin-polarization energy of a Si atom which has been calculated to be -0.62 eV [S. H. Lee, J. H. Kang, and M. H. Kang, J. Korean Phys. Soc. **31**, 811 (1997)]. Consideration of it gives a uniform downward shift in the adsorption energies.

[24] In fact, we need an additional PES where the adatom geometries possess broken backbonds [see, e.g., Figs. 2(b) and 2(c)].

[25] Structures around $x_{\mathrm{H}} = 0.5$ Å [open and filled circles, and open and filled squares in Fig. 3(a)] are all similar to Fig. 2(b): a common feature that the Si4-Si5 backbond is broken.

[26] The brokenback bond is not strange if we consider that the corresponding bond length (2.87 Å) in the B^0 geometry [Fig. 1(c)] is much larger than the bulk value, 2.35 Å. When the adatom is located around site B, the subsurface Si atom (Si5) and dimer atoms (Si2 and Si4) all become fivefold coordinated, and the bond strengths thus weaken significantly.

[27] Y. W. Mo, J. Kleiner, M. B. Webb, and M. G. Lagally, Phys. Rev. Lett. **66**, 1998 (1991).

[28] J. D. Wrigley and G. Ehrlich, Phys. Rev. Lett. **44**, 661 (1980).

[29] G. L. Kellogg and P. J. Feibelman, Phys. Rev. Lett. **64**, 3143 (1990).

[30] C. Chen and T. T. Tsong, Phys. Rev. Lett. **64**, 3147 (1990).

[31] P. J. Feibelman, Phys. Rev. Lett. **65**, 729 (1990).

[32] B. D. Yu and M. Scheffler, Phys. Rev. B **56**, R15 569 (1997).

[33] K. C. Pandey, Phys. Rev. Lett. **57**, 2287 (1986).

[34] M. V. R. Murty and H. A. Atwater, Surf. Sci. **374**, 283 (1997).

[35] L. Patthey, E. L. Bullock, T. Abukawa, S. Kono, and L. S. O. Johansson, Phys. Rev. Lett. **75**, 2538 (1995).

[36] H. W. Yeom, M. Sasaki, S. Suzuki, S. Sato, S. Hosoi, M. Iwabuchi, K. Higashiyama, H. Fukutani, M. Nakamura, T. Abukawa, and S. Kono, Surf. Sci. **381**, L533 (1997).

[37] In their recent paper, Nara, Sasaki, and Ohno considered a dihydride structure where the adatom is located at T_1 (above the center of a dimer) and obtained the barriers of 1.5 and 1.7 eV for adatom diffusion parallel and perpendicular to the dimer rows, respectively [Phys. Rev. Lett. **79**, 4421 (1997)]. However, they did not deal with the exchange mechanism for the adatom diffusion. Except for the above two points, the overall results of their paper agree with present ones: spontaneous substitutional adsorption, diffusion mechanisms of H release and capture, etc.